

# Data Assimilation and Parameter Estimation for the Global Ionosphere-Thermosphere Model using the Ensemble Adjustment Kalman Filter

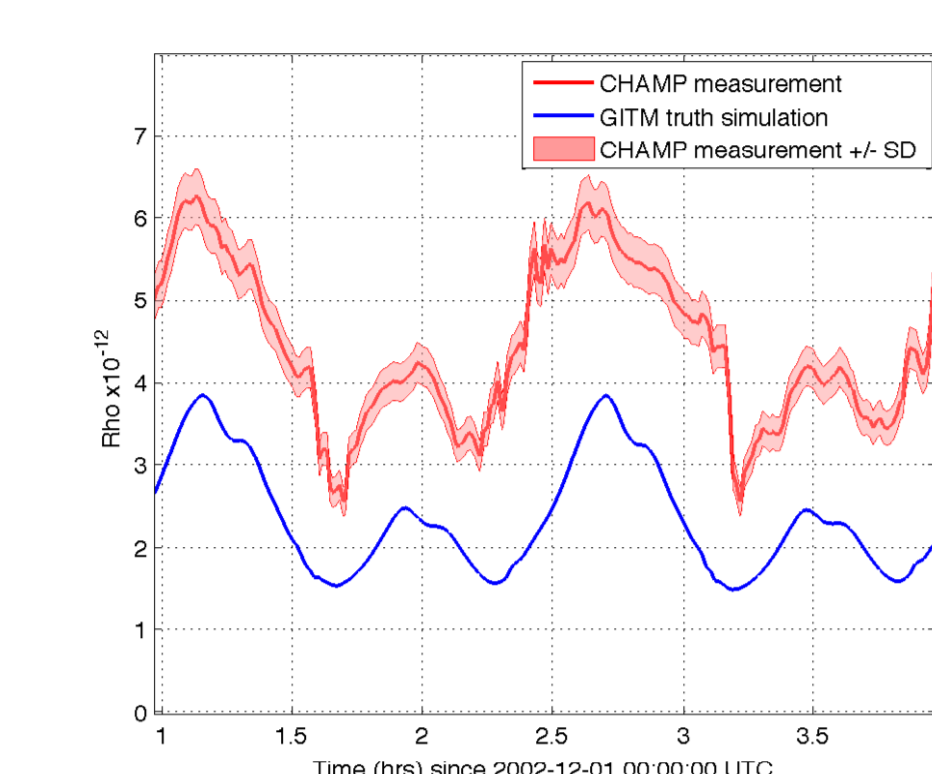
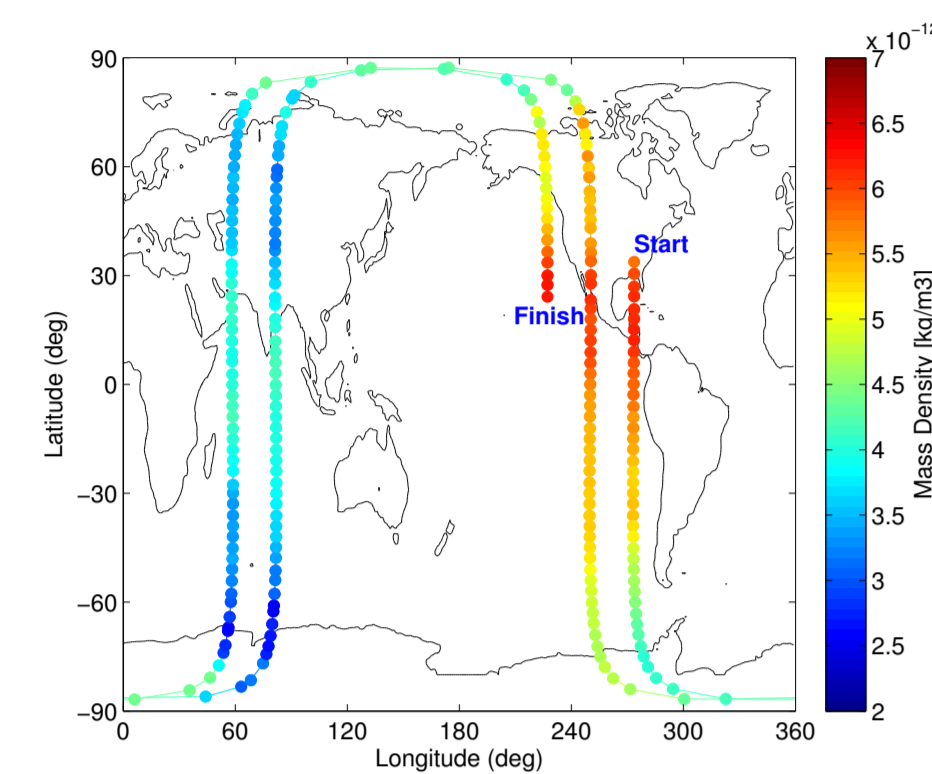
Alexey V. Morozov, Aaron J. Ridley, Dennis S. Bernstein - University of Michigan, Ann Arbor, MI

Nancy Collins, Timothy J. Hoar, Jeffrey L. Anderson - National Center for Atmospheric Research, Boulder, CO



## Introduction

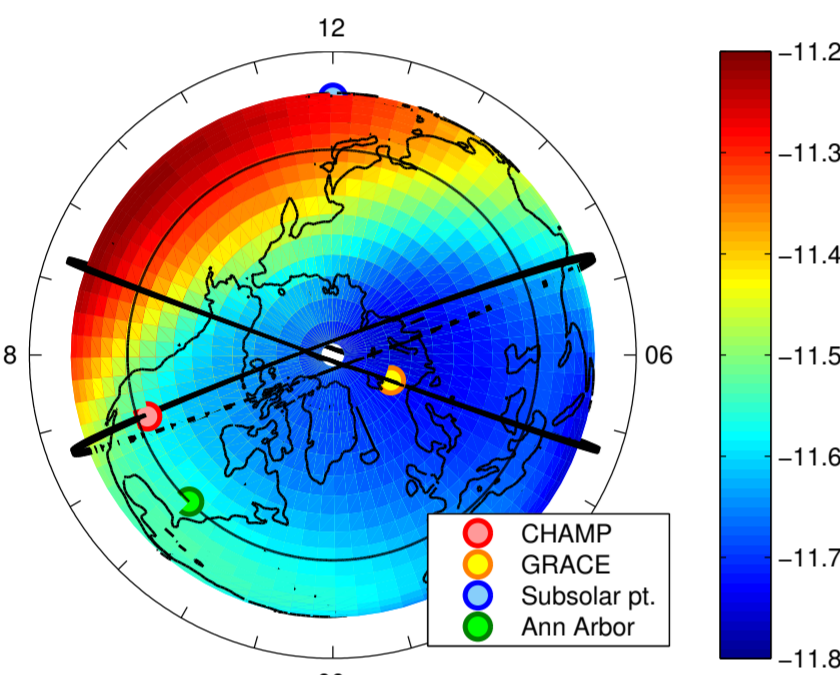
- GITM underestimates mass density when compared with CHAMP measurements.
- One way to correct this is to use CHAMP measurements to estimate GITM parameters that would compensate for modeling error.
- One approach is EAKF, which is part of the Data Assimilation Research Testbed (DART).



CHAMP measures mass density ( $\rho$ ).

GITM underestimates  $\rho$  at CHAMP locations.

## Model



Dawn-dusk diagram showing CHAMP and GRACE orbits, as well as Ann Arbor and subsolar point. Color represents  $\rho$  at 400km at 02:32 UT.

### Global Ionosphere-Thermosphere Model (GITM)

- is an upper atmosphere model,
- is a contractive system (*i.e.* strongly forced),
- does not assume a hydrostatic solution, and
- does not use a pressure-based coordinate system.

The last two features allow for more realistic physics in auroral region.

## GITM: Inputs and Outputs

### Inputs (parameters)

- Solar flux index  $F_{10.7} \rightarrow$
- Cooling rates  $L_c \rightarrow$
- Heating efficiency  $\epsilon \rightarrow$
- Thermal conductivity  $\kappa_c \rightarrow$
- ...

### Outputs

- $\rightarrow N_s$  Neutral number densities
- $\rightarrow \rho$  Neutral mass density
- $\rightarrow p$  Neutral pressure
- $\rightarrow \mathcal{T}$  Neutral temperature normalized
- $\rightarrow \mathbf{u}$  Neutral velocity
- $\rightarrow N_j$  Ion number densities
- $\rightarrow T_j$  Ion temperature normalized
- $\rightarrow \mathbf{v}$  Ion velocity

## GITM: Vertical Equations

- Vertical solver accounts for all the source terms.
- Vertical continuity, momentum, and temperature equations are

$$\frac{\partial \mathcal{N}_s}{\partial t} + \frac{\partial u_{r,s}}{\partial r} + \frac{2u_{r,s}}{r} + u_{r,s} \frac{\partial \mathcal{N}_s}{\partial r} = \frac{1}{N_s} \mathcal{S}_s, \quad (1)$$

$$\frac{\partial u_{r,s}}{\partial t} + u_{r,s} \frac{\partial u_{r,s}}{\partial r} + \frac{u_\theta \partial u_{r,s}}{r \partial \theta} + \frac{u_\phi \partial u_{r,s}}{r \cos(\theta) \partial \phi} + \frac{k \partial T}{M_s \partial r} + \frac{kT \partial \mathcal{N}_s}{M_s \partial r} =$$

$$g + \mathcal{F}_s + \frac{u_\theta^2 + u_\phi^2}{r} + \cos^2(\theta) \Omega^2 r + 2 \cos(\theta) \Omega u_\phi, \quad (2)$$

$$\frac{\partial \mathcal{T}}{\partial t} + u_r \frac{\partial \mathcal{T}}{\partial r} + (\gamma - 1) \mathcal{T} \left( \frac{2u_r}{r} + \frac{\partial u_r}{\partial r} \right) = \frac{k}{c_v \rho \bar{m}_n} \mathcal{Q}, \quad (3)$$

$$\mathcal{Q} = Q_{\text{EUV}} + Q_{\text{NO}} + Q_{\text{O}} + \frac{\partial}{\partial r} \left( \kappa_c + \kappa_{\text{eddy}} \right) \frac{\partial T}{\partial r} + N_e \frac{\bar{m}_i \bar{m}_n}{\bar{m}_i + \bar{m}_n} \nu_{\text{in}} (\mathbf{v} - \mathbf{u})^2, \quad (4)$$

$$Q_{\text{EUV}} = \sum_s \sum_\lambda \left[ N_s(z) I_\infty(\lambda) e^{-\sec(\chi) \sum_s N_s(z) \sigma_s^a(\lambda) H_s(z)} \right], \quad (5)$$

$$I_\infty(\lambda) = f(\lambda) \left[ 1 + a(\lambda) \left( \frac{F_{10.7}}{2} + \left( \frac{F_{10.7}}{2} \right)^{1.5} \right) \right],$$

## EAKF

- First, define joint state-measurement vector as  $z_k = \begin{bmatrix} x_k \\ y_k \end{bmatrix}$ .
- Then,  $N$  EAKF ensemble members can be updated via

$$\hat{z}_{k,i}^- = [f_{k-1}(\hat{x}_{k-1,i}^+, u_{k-1}, 0); h_k(\hat{x}_{k-1,i}^+, 0)], \quad (6)$$

$$\mathcal{P}_k^- = \sum_{i=1}^N (\hat{z}_{k,i}^- - \mu \hat{z}_k^-) (\hat{z}_{k,i}^- - \mu \hat{z}_k^-)^T / (N - 1), \quad (7)$$

$$\mathcal{A}_k = (\mathcal{F}_k^T)^{-1} \mathcal{G}_k^T (U_k^T)^{-1} B_k^T (\mathcal{G}_k^T)^{-1} \mathcal{F}_k^T, \quad (8)$$

$$\mathcal{P}_k^+ = [(\mathcal{P}_k^-)^{-1} + \mathcal{H}^T R_k^{-1} \mathcal{H}]^{-1}, \quad (9)$$

$$\mu \hat{z}_k^+ = \mathcal{P}_k^+ [(\mathcal{P}_k^-)^{-1} \mu \hat{z}_k^- + \mathcal{H}^T R_k^{-1} y_k], \quad (10)$$

$$\hat{z}_{k,i}^+ = \mathcal{A}_k^T (\hat{z}_{k,i}^- - \mu \hat{z}_k^-) + \mu \hat{z}_k^+. \quad (11)$$

where

- $\mathcal{F}_k$  comes from SVD of  $\mathcal{P}_k^- = \mathcal{F}_k D_k \mathcal{F}_k^T$ .
- $\mathcal{G}_k$  is a square root of  $D_k$ , as in  $\mathcal{G}_k = D_k^{1/2}$ .
- $U_k$  comes from SVD of  $\mathcal{G}_k^T \mathcal{F}_k^T \mathcal{H}^T R_k^{-1} \mathcal{H} \mathcal{F}_k \mathcal{G}_k = U_k J_k U_k^T$ .
- $B_k$  is a square root of  $B_k$ , as in  $B_k = (I + J_k)^{-1/2}$ .

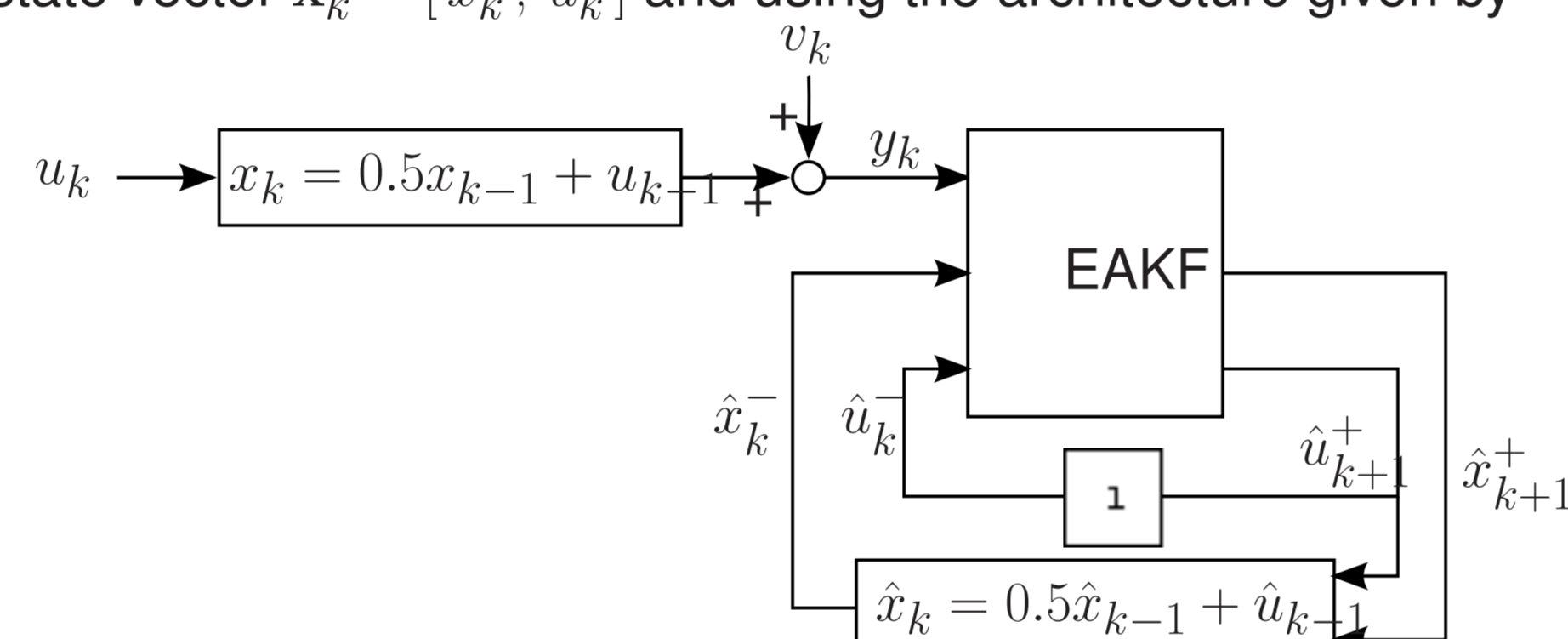
## Example: Estimating a Time-Varying Parameter

- Consider the linear system

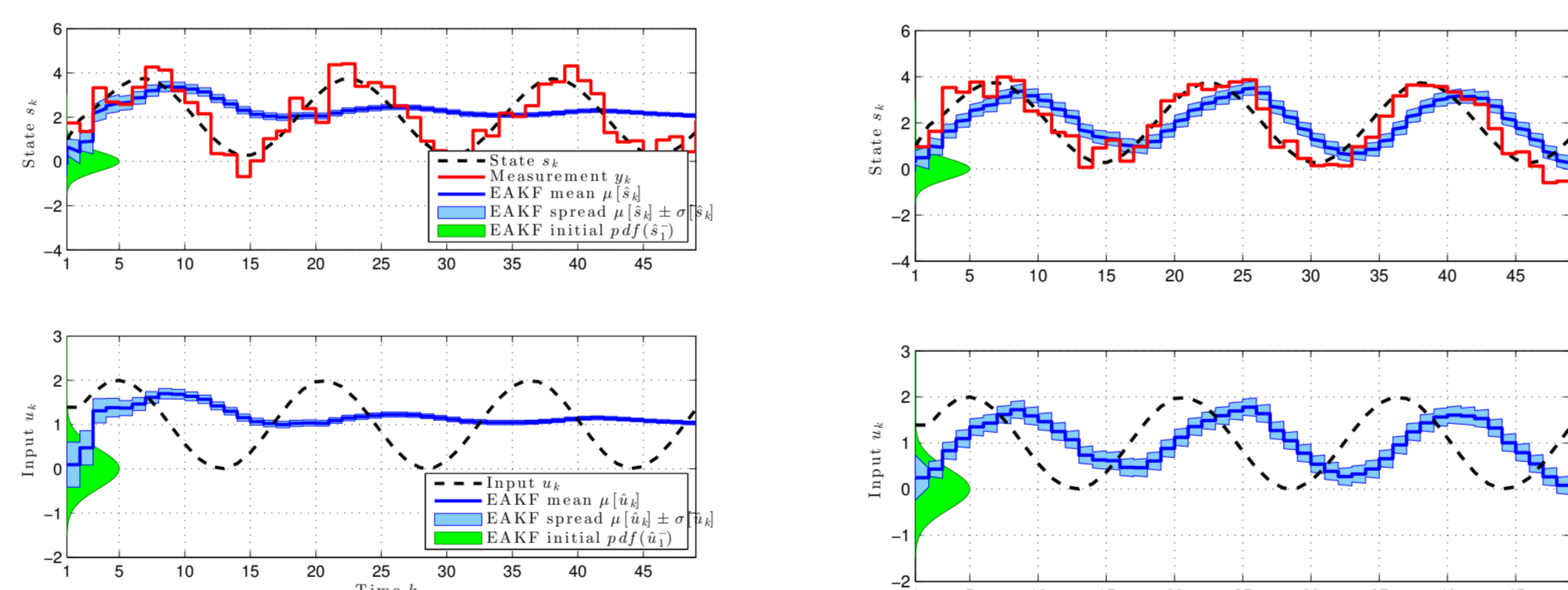
$$x_k = 0.5x_{k-1} + u_{k-1}, \quad u_k = 1.0 + \sin(0.5k), \quad (12)$$

$$y_k = x_k + v_k, \quad v_k \sim N(0, 0.2). \quad (13)$$

- Input (driver, parameter)  $u_k$  can be estimated by augmenting the state vector  $x_k = [x_k; u_k]$  and using the architecture given by



- Example without and with parameter inflation:



Absence of measurements of the input  $u_k$  (top plot) results in filter divergence (ensemble spread ( $\sigma[\hat{u}_k]$  and  $\sigma[\hat{x}_k]$ ) goes to zero and ensemble mean deviates away from the true input and state).

Using parameter variance inflation

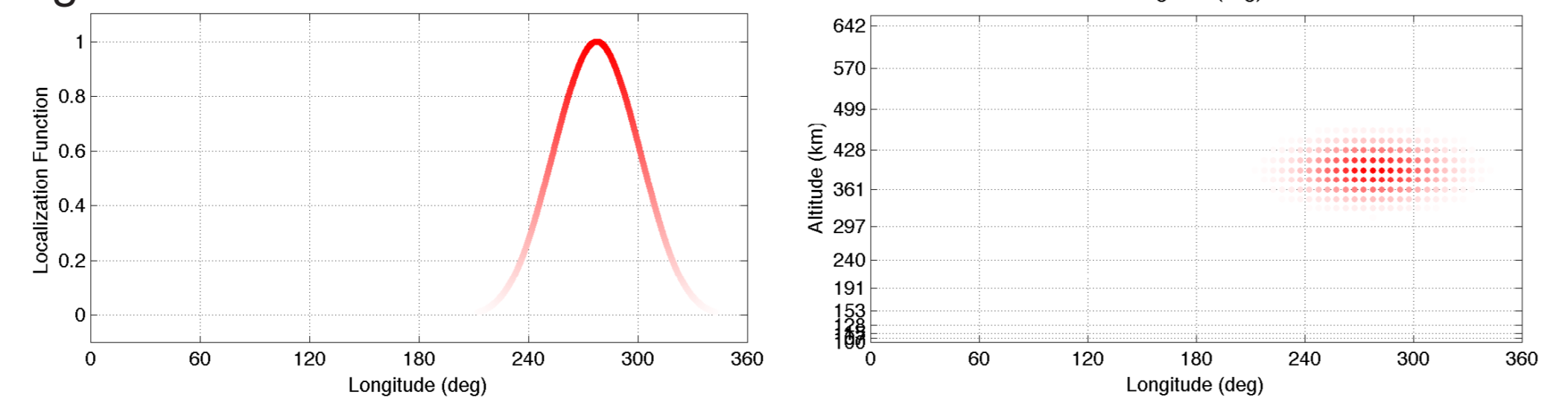
$$\hat{u}_{k,i}^- = \sqrt{\frac{\sigma_i^2}{\sigma^2[\hat{u}_k^-]} (\hat{u}_{k,i}^- - \mu[\hat{u}_k^-]) + \mu[\hat{u}_k^-]}$$

with  $\sigma_i = 0.2$  improves performance.

## Localization

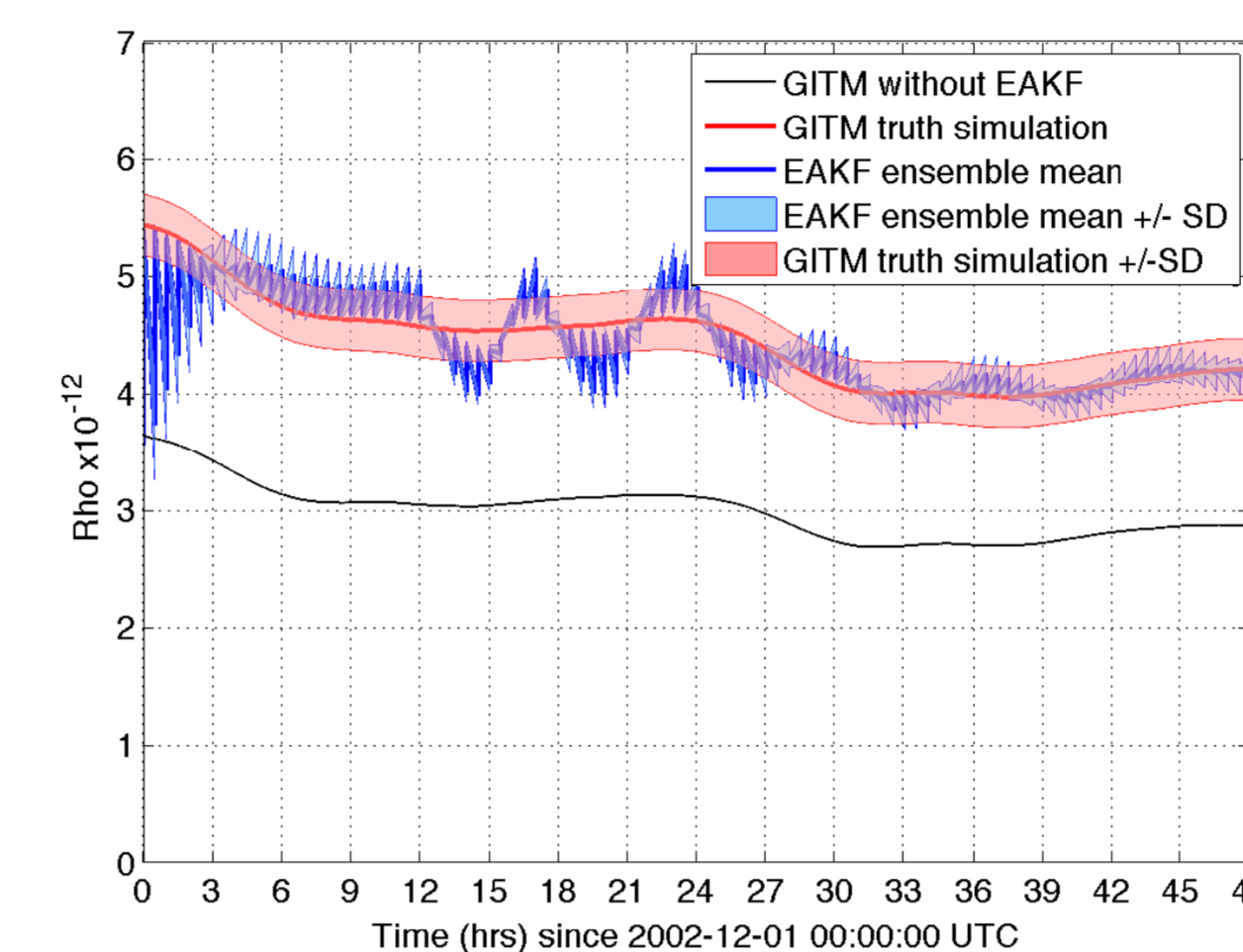
- The effect of assimilation can be restricted to a region to avoid updating uncorrelated states.

Localization function with horizontal cutoff of  $30^\circ$  is shown to the right and below, and vertical cutoff of  $100\text{km}$  is shown bottom right.

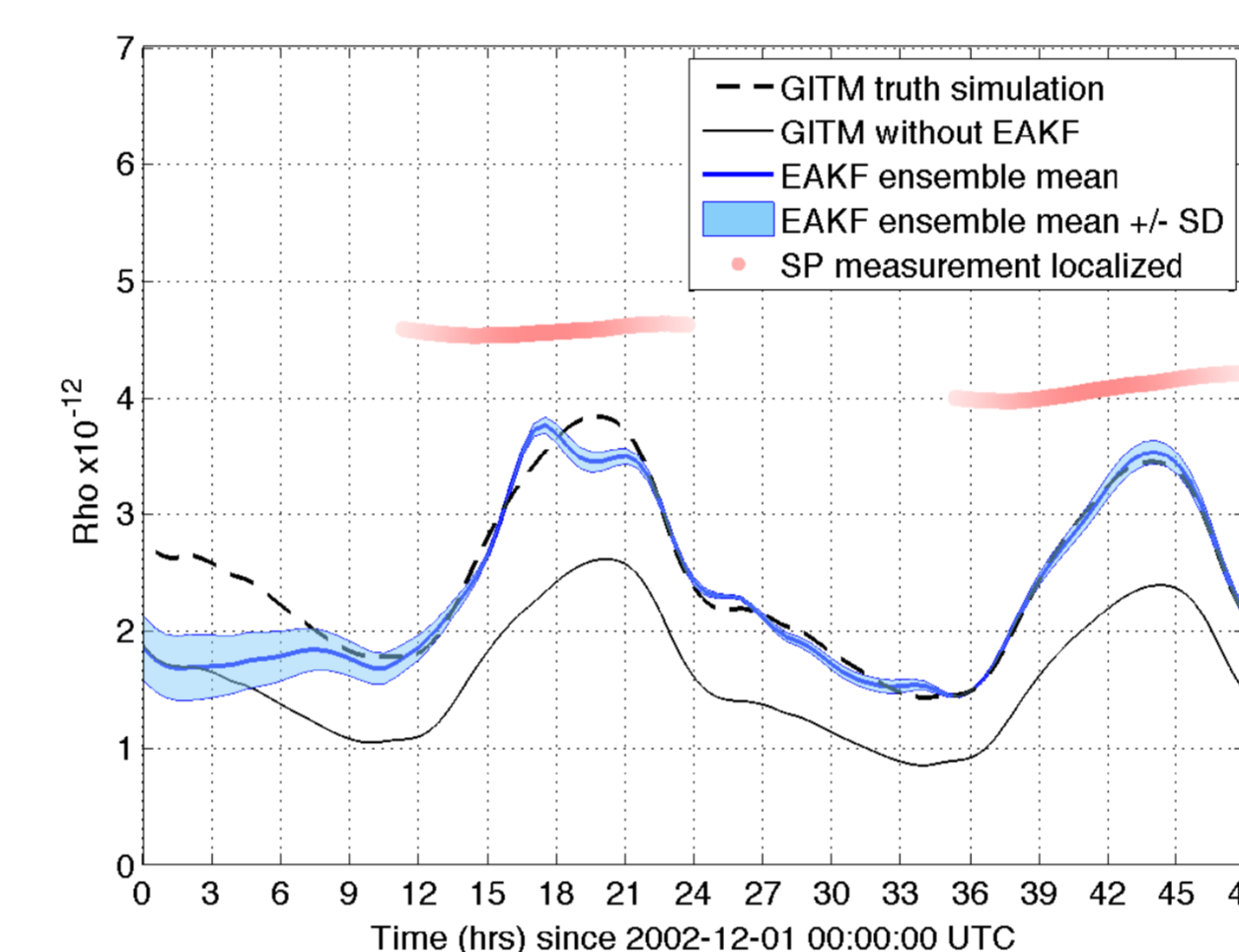


## Results: Simulated Data from Subsolar Point

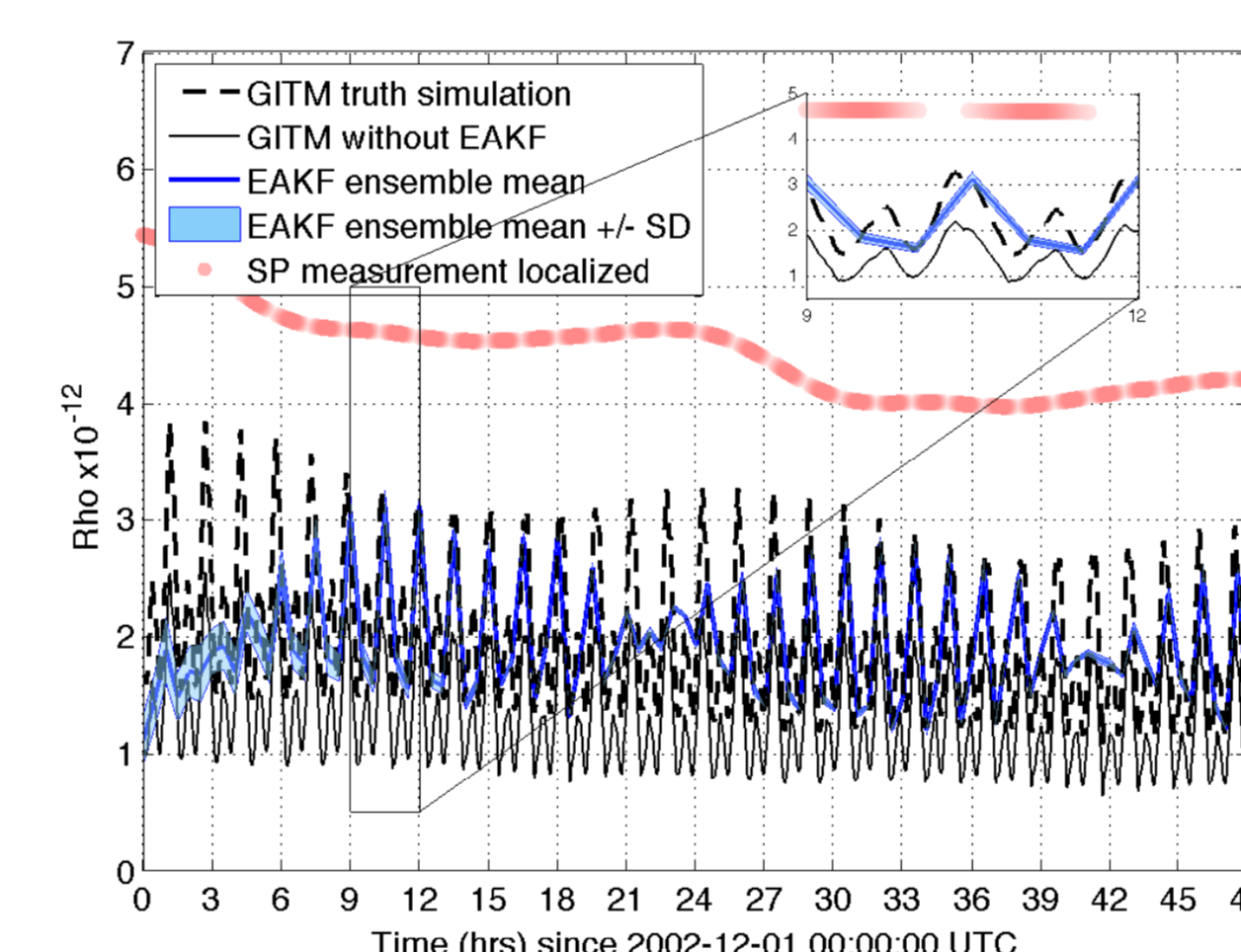
- The introductory example is a perfect model experiment, *i.e.* it takes measurements from a GITM truth simulation with  $F_{10.7}$  fixed at 150.
- EAKF assimilation window is 30 minutes, measurements are available every 1 minute, horizontal cutoff of  $30^\circ$ , and vertical cutoff of  $100\text{km}$ .
- 20 ensemble members are prespun for 2 days prior to Dec 01 with  $F_{10.7}$  values coming from normal distribution  $\sim N(130, 25)$ .
- $\hat{F}_{10.7}$  is inflated using  $\sigma_i = 7$ .



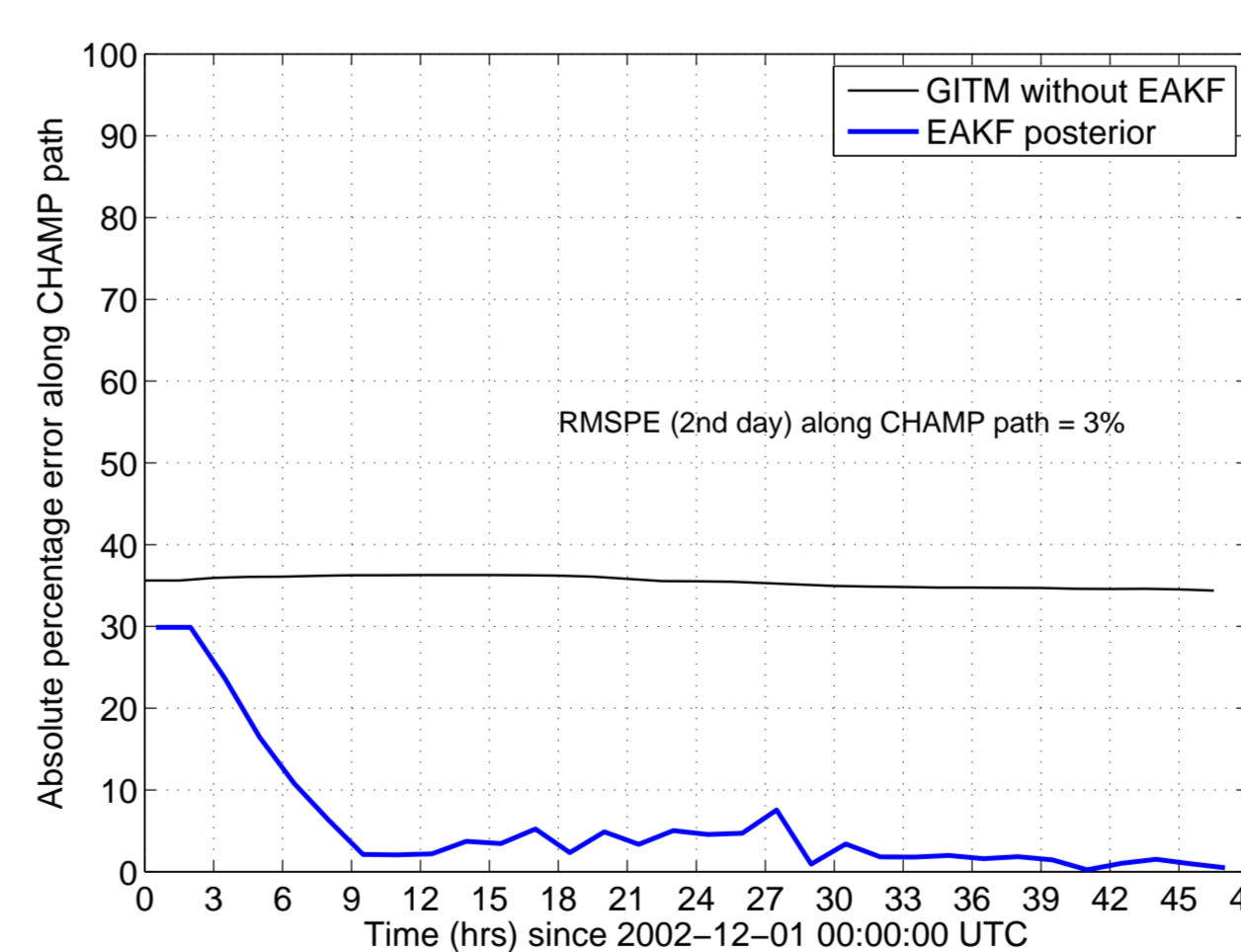
$\rho$  estimates at subsolar point (measurement location). We assume measurement error variance ( $R$ ) for  $\rho$  to be  $2.6 \times 10^{-13} \text{kg/m}^3$  (an average value taken from real CHAMP data uncertainty for the two days in question).



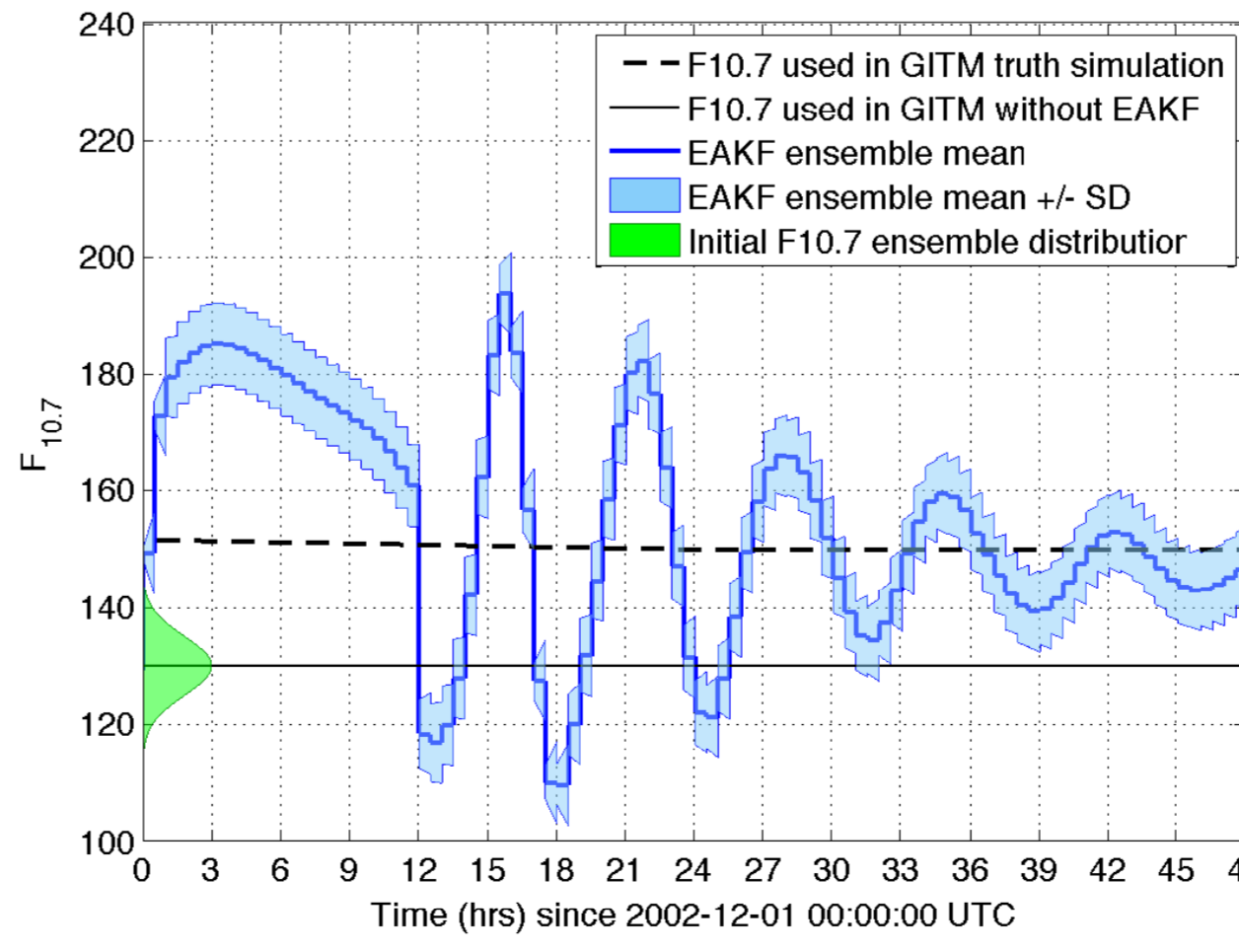
$\rho$  estimates 400km above Ann Arbor, MI. Here  $\rho$  estimates approach the truth data, but only when subsolar point measurements are "close" to Ann Arbor (localization cutoff is tripled in this and the next plot to demonstrate periods of proximity).



$\rho$  at CHAMP location (diagnostic location). This figure demonstrates that initially EAKF underestimates  $\rho$  at CHAMP location, but the estimates improve as time increases (this can be seen more explicitly in the next plot).



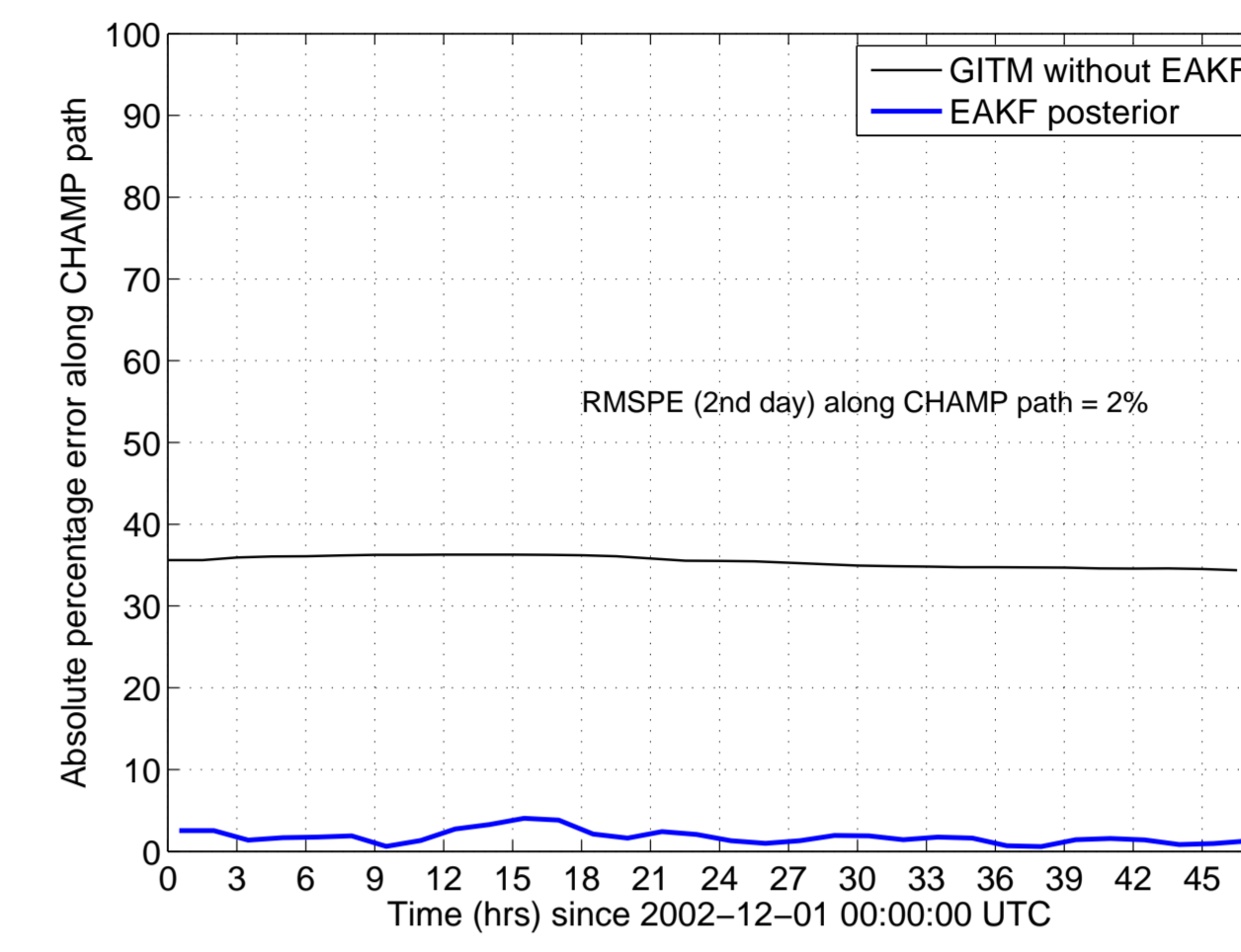
Root mean square percentage error (RMSPE) in  $\rho$  along CHAMP orbit averaged over 90 minutes. We define  $\text{RMSPE} \triangleq \frac{\sqrt{(\rho - \hat{\rho})^2}}{\rho}$ . RMSPE for the second day along CHAMP track in this case is computed to be about 3%.



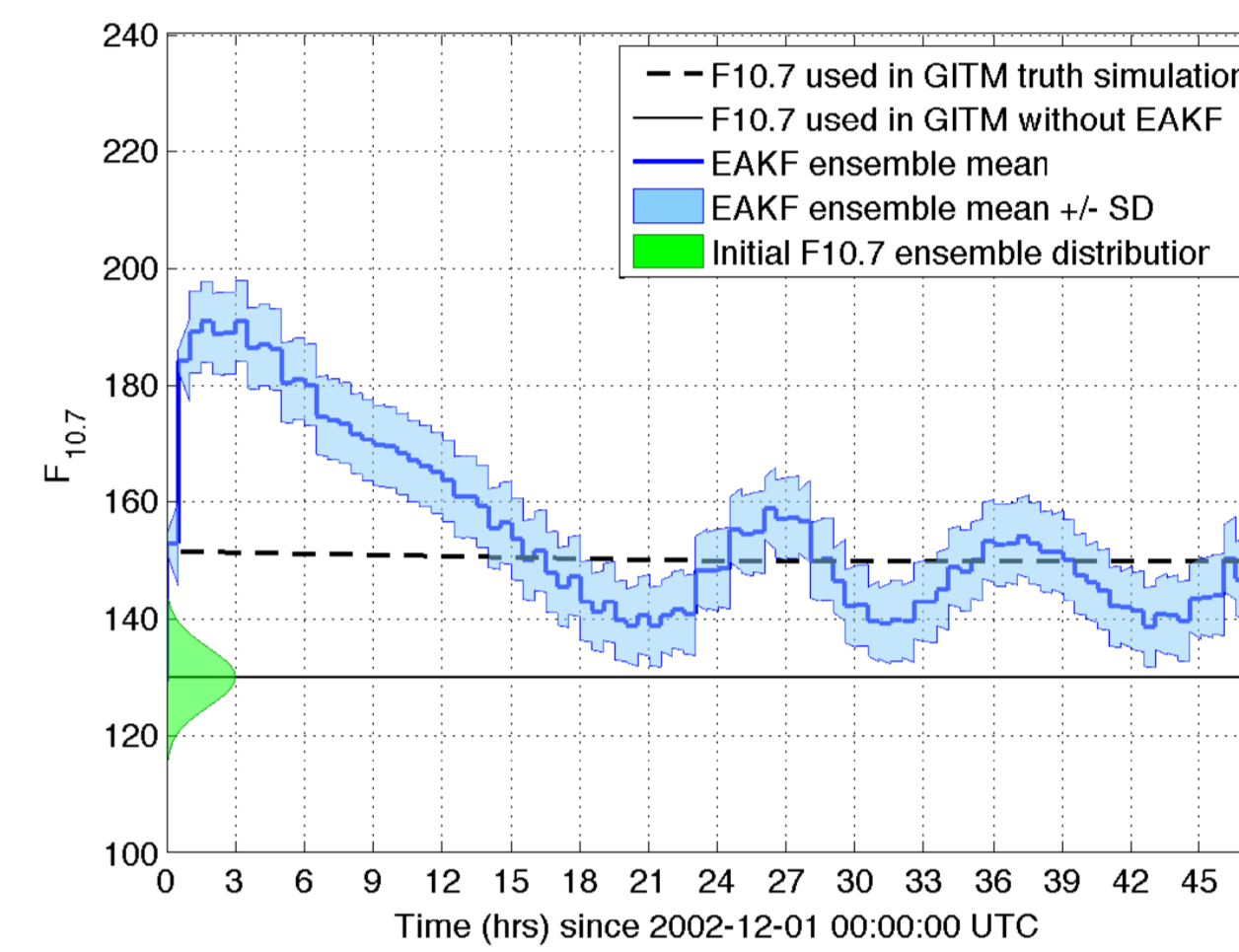
$F_{10.7}$  estimate. After starting from initial distribution centered about 130 (stretched horizontally for demonstrational purposes), EAKF ensemble mean approaches the true value.

## Simulated Data from CHAMP

- This example is also a perfect model experiment.
- 20 ensemble members are prespun for 2 days prior to Dec 01 with  $\hat{F}_{10.7}$  values coming from normal distribution  $\sim N(130, 25)$ .
- $\hat{F}_{10.7}$  is inflated using  $\sigma_i = 7$ .



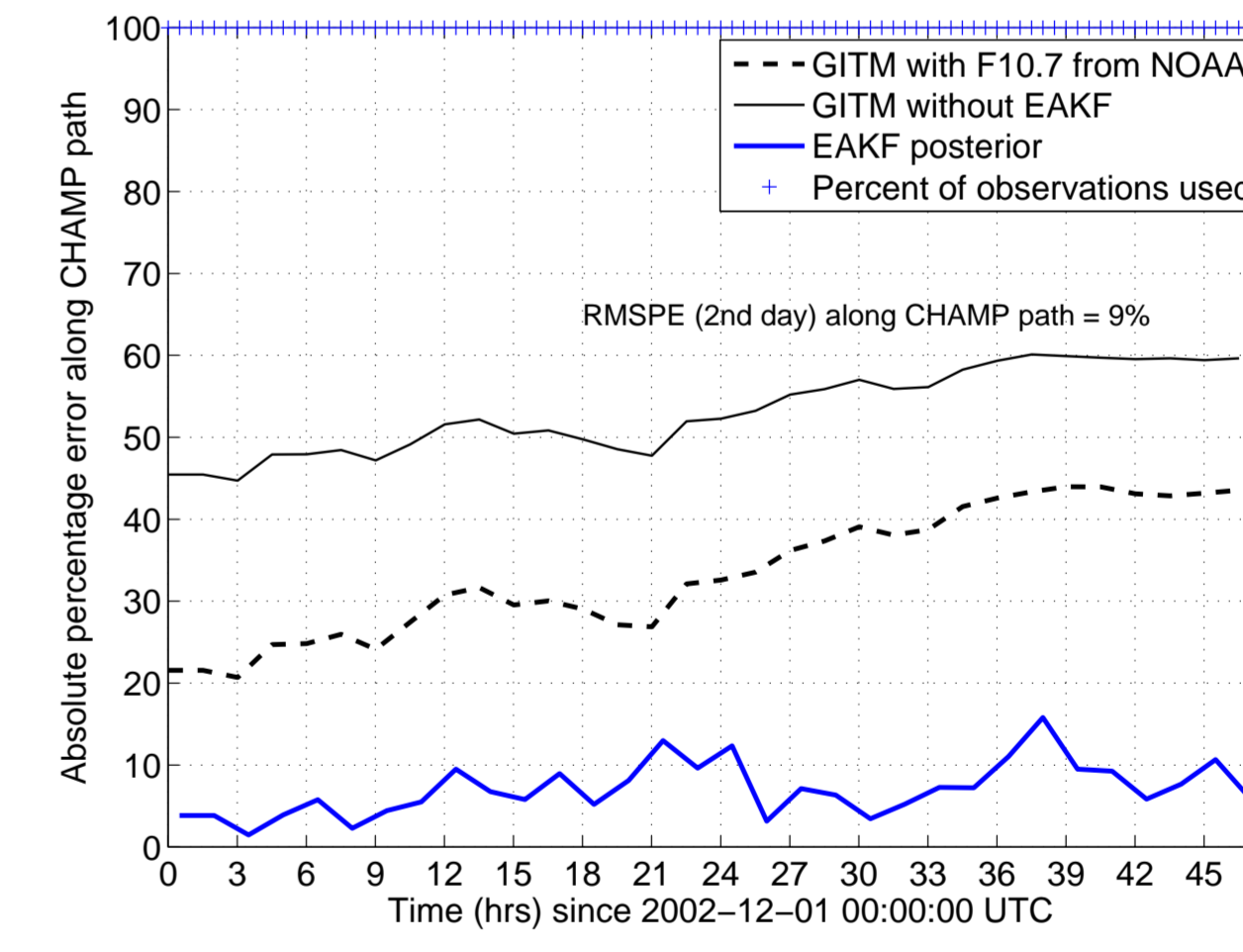
$\rho$  RMSPE along CHAMP orbit averaged over 90 minutes. RMSPE for the second day along CHAMP track in this case is computed to be about 2%.



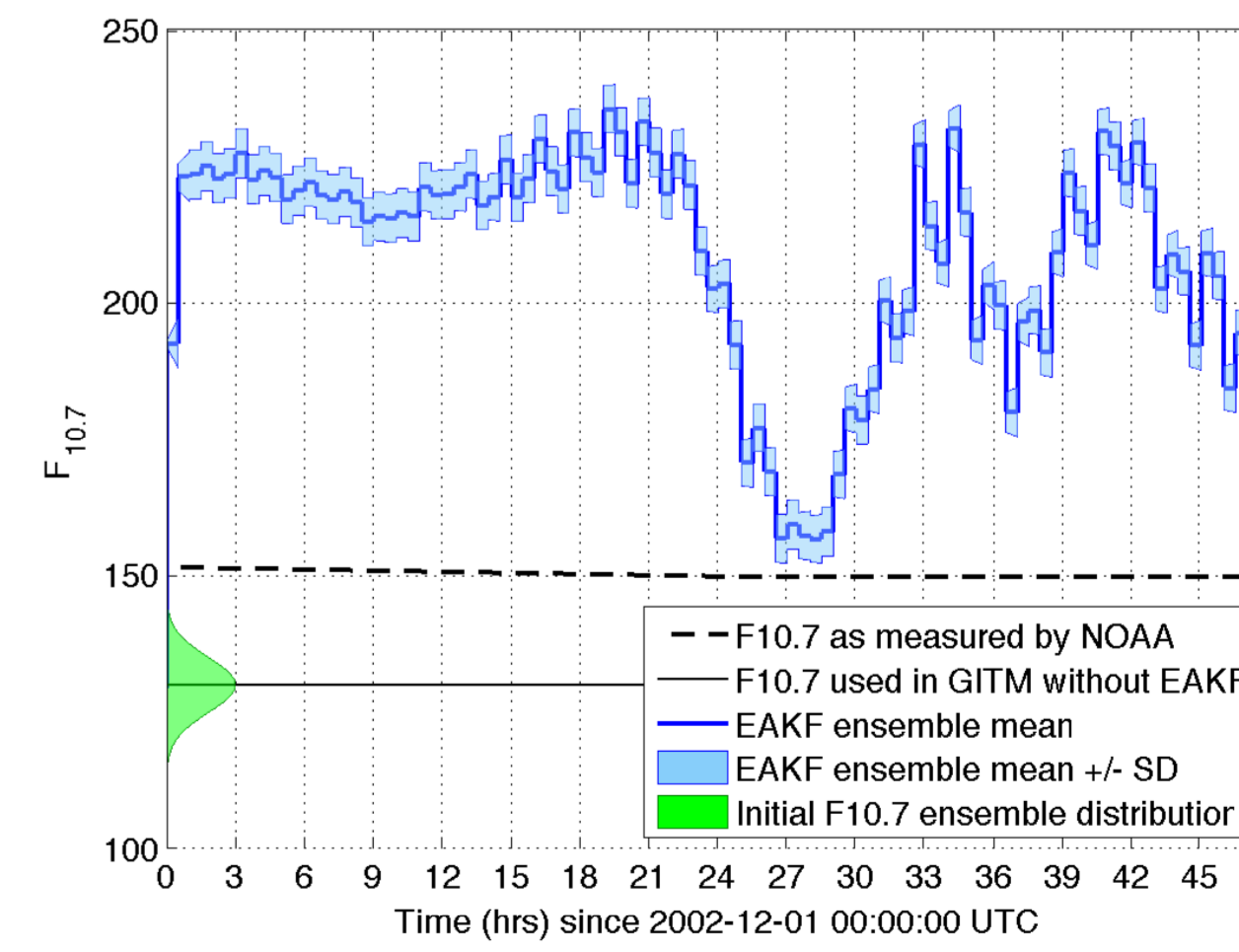
$F_{10.7}$  estimate. After starting from initial distribution centered about 130, EAKF ensemble mean approaches the true value.

## Real Data from CHAMP

- This example draws its measurements from real CHAMP data.
- 20 ensemble members are prespun for 2 days prior to Dec 01 with  $\hat{F}_{10.7}$  values coming from normal distribution  $\sim N(130, 25)$ .
- $\hat{F}_{10.7}$  is inflated using  $\sigma_i = 4.47$ .



Here,  $\rho$  RMSPE along CHAMP orbit is defined as  $\text{RMSPE} \triangleq \frac{\sqrt{(\rho_{\text{CHAMP}} - \hat{\rho})^2}}{\rho_{\text{CHAMP}}}$  and is computed for  $\rho$  the mean case ( $F_{10.7} = 130$ ) to be 58%, the NOAA case ( $F_{10.7} = 150$ ) - 41%, the EAKF case - 9%.



Here, the  $F_{10.7}$  estimate does not converge to the NOAA-measured value of 150, but instead compensated for model mismatch.

## Conclusions and Future Work

- EAKF was successfully used to estimate GITM states ( $N_s, N_j, \mathcal{T}, T_j, \mathbf{u}, \mathbf{v}$ ) and a parameter ( $F_{10.7}$ ) using CHAMP  $\rho$  measurements.
- One proposed extension is estimating the full solar spectrum at the top of the atmosphere ( $I_\infty(\lambda)$ ).
- Another possible extension is using Total Electron Content (TEC) measurements to estimate heating efficiency ( $\epsilon$ ).